A Comparative Study of Gadolinium Gallium Garnet Growth by Femtosecond and Nanosecond Pulsed Laser Deposition

M. S. B. Darby, T. C. May-Smith and R. W. Eason

Optoelectronics Research Centre, University of Southampton, Southampton, SO17 1BJ, United Kingdom

T. Donnelly and J. G. Lunney

School of Physics, Trinity College Dublin, Dublin 2, Ireland

K. D. Rogers

Department of Materials & Medical Sciences, Cranfield University, Shrivenham, Swindon, SN6 8LA, United Kingdom

Abstract

The growth of epitaxial Nd:$G_3Ga_5O_{12}$ (GGG) on $Y_3Al_5O_{12}$ (YAG) by femtosecond pulsed laser deposition is reported. We have used a Ti:sapphire laser at a wavelength of 800 nm and pulse length of 130 fs, operating at a repetition rate of 1 kHz. The film properties have been studied systematically as a function of the deposition parameters of laser fluence, spot-size, oxygen pressure, target-substrate distance and temperature. Scanning electron microscopy, atomic force microscopy and X-ray diffractometry were used to characterise the surface structure and crystallinity of the films. X-ray diffraction analysis shows that epitaxial growth has occurred and also

confirms that the films are single crystal. A comparison between the ion velocities produced by nanosecond and femtosecond laser ablation of the GGG target material has been investigated by the Langmuir probe technique. The results indicate a large difference in the plasma characteristics between femtosecond and nanosecond ablation, with ion velocities up to eight times faster observed in the femtosecond case.

Key words: pulsed laser deposition, plasmas, femotsecond, Lagmuir probe, thin films, garnet crystal, epitaxy

PACS: 68.55.jk, 81.15.-z, 77.55.+f, 52.27.Cm

1 Introduction

The study of nanosecond pulsed laser deposition (PLD) and plasmas has been prevalent over the past 20 years and has found numerous applications with a diverse range of materials [1]. With the recent advent of high energy, high repetition rate sub-picosecond lasers there is the opportunity to investigate this technique in the short temporal regime. Research on the subject of PLD using short pulse duration lasers has increased in popularity recently, and there have been several reports over the past few years demonstrating the potential of this technique. High pulse-rate (76 MHz) picosecond lasers have been used to deposit chalcogenide [2] and carbon films [3] with a consequent elimination of the particulate contamination normally seen with nanosecond lasers. Femtosecond PLD of $BaTiO_3$ [4] at a wavelength of 620 nm reveals coalesced particles up to 1 μm in size with poor crystallinity and high surface roughness. Thin films of GaAs have been deposited with varying pulse du-

Email address: msbd@orc.soton.ac.uk (M. S. B. Darby,).

rations and show the formation of nanoclusters [5]. Femtosecond deposition of polytetrafluoroethylene (PTFE) on single crystal silicon wafers using an 800 nm wavelength laser has been shown to produce films with lower particulate density, more efficient stoichiometric transfer of target material and with a smoother surface compared to excimer laser-deposited films [6].

The high laser intensities ($\sim 10^{13}$ Wm^2) available with femtosecond lasers means that the dominant mechanisms for laser-matter interaction are multiphoton absorption and avalanche ionization [7, 8], which permits laser ablation at wavelengths that would not be possible via single photon absorption in the nanosecond regime. The electrons produced by avalanche ionization dominate the absorption by Bremsstrahlung and resonance absorption, and the mechanisms of the laser absorption become independent of the initial state of the target [7–9]. The femtosecond pulse interaction process takes place when the laser pulse duration is shorter than characteristic thermal relaxation times and therefore thermal damage around the ablation area is significantly reduced.

This paper reports the properties of Nd:$G_3Ga_5O_{12}$ (GGG) films deposited with femtosecond laser pulses for a wide range of experimental conditions and investigates the ion velocities of the laser-produced plume in both the nanosecond and femtosecond regimes using the Langmuir probe technique. We contrast our findings with GGG fabricated by a nanosecond UV excimer laser [10] and make a comparative study.

2 Experimental

The experiments were conducted in a vacuum chamber with an oxygen ambient gas pressure ranging between 10^{-4} mbar and 10^{-1} mbar. A Ti:sapphire laser was used to ablate the target material with 130 fs pulses at a wavelength of 800 nm operating at a repetition rate of 1 kHz. The target material was ablated with single pulse energies which varied from 0.1 to 1.2 mJ. Experiments were conducted for a range of spot-sizes (elliptical in shape due to the 45° angle of incidence used) ranging from 32 μm by 45 μm to 135 μm by 195 μm corresponding to fluence values ranging from 1.3 to 19 J/cm^2. Trial depositions were conducted for a duration of 10 minutes using an undoped GGG target and once the conditions for epitaxial growth were established, films were grown for successively longer durations using a Nd:GGG (1% doped) target. The target was rotated spirographically in order to increase the usable target area during a given deposition run. This is an important point compared to typical nanosecond depositions, as the focussed spot-size for femtosecond deposition is a few orders of magnitude smaller than for nanosecond PLD. An associated and also important factor here concerns the use of continuous motors and spirographic rotation for femtosecond PLD compared to the more usual stepper motor and circular rotation drive for nanosecond PLD: the two orders of magnitude increase in the laser repetition rate (1 kHz for femtosecond compared to 10 Hz for nanosecond) effectively prohibits circular rotation and stepper drive motors. The small ablation area means that ablation channels are rapidly formed on the target material if the target is rotated about a single axis.

The substrates were heated using a 25 W 10.6 μm wavelength CO_2 laser, with

the Gaussian beam homogenized onto a 1 cm × 1 cm square substrate either using a brass reflective beam-pipe or a tetra-prism [11]. The temperature of the substrates was calibrated using a thermocouple attached to the surface of a test $Y_3Al_5O_{12}$ (YAG) substrate. Indium metal was used to improve conductivity between the thermocouple and the substrate. The substrates were mounted using ceramic alumina holders to minimize any undesirable localised heat-sinking. The target-substrate distance was set to either 2.5, 3, or 4.5 cm. A remotely controlled substrate-shutter was used to prevent the plume from reaching the substrate during pre-deposition ablative cleaning of the target surface. The spot-size, and hence the incident laser fluence, was initially measured by ablating a silicon wafer with a fixed energy and measuring the damaged region under an optical microscope. More accurate measurements of the spot-size were taken using the knife-edge technique. The deposition chamber was evacuated to a pressure below 10^{-4} mbar prior to deposition, and oxygen was then continuously introduced into the chamber to maintain the desired pressure for each experiment.

A Bruker D8 X-ray diffractometer with general area detector diffraction system (GADDS) was initially used to assess the crystallographic quality of the films. This provided diffraction data from an extended region of reciprocal space and therefore enabled rapid and unambiguous discrimination between highly textured and epitaxial films (both of which could produce single Bragg peaks when measured in the conventional $\theta/2\theta$ mode). Films were examined using CuKα radiation and a monocapillary with diameter $\approx 50\,\mu$m. A film was also examined in a line-scan mode, where a series of diffraction patterns were recorded at a number of different positions across the sample to assess homogeneity. Subsequently a Siemens D5000 X-ray diffractometer was used

(CuKα radiation) for X-ray diffraction analysis of all the Nd:GGG or GGG films grown. A LEO 1455VP SEM and an Explorer AFM were used to analyze the topography of the films.

The ion emission flux of the plasma was characterised by means of a planar Langmuir probe at a distance of 2.5 or 4 cm from the target surface. The probe consisted of a copper plate of dimension 2×5 mm^2 for nanosecond ablated ion characterisation and 2.5×5 mm^2 for femtosecond ablated ion characterization. For each measurement the probe was biased at -30 V, and the collected ion current was determined by the voltage signal recorded on a digital oscilloscope across a load resistor (10 Ω). The bias was maintained using a 1.2 μF capacitor, which was sufficient to avoid charge saturation. A diagram of a typical probe circuit (used for measurements of femtosecond ablated ions) is shown in Fig. 1. The Nd:GGG target, placed on a rotating target holder, was ablated under oxygen pressure of 10^{-1} mbar to 10^{-4} mbar. The time of incidence of the laser pulse was measured using a photodiode and was also confirmed by the detection of a photo-peak from the Langmuir probe. Langmuir probe measurements of nanosecond ablated ions were carried out in a second chamber with a base pressure of 10^{-5} mbar. To compare the plume characteristics with the nanosecond regime, a KrF excimer laser operating at a wavelength of 248 nm, pulse duration of ≈ 25 ns and pulse energy of 50 mJ was used, with a laser spot-size of 1 mm $\times$4 mm. For measurements of ion signals for both the femtosecond and nanosecond regimes the laser was operated on single-shot mode.

3 Results and discussion

The initial examination using the GADDS area detector produced strong evidence for the epitaxial nature of the films examined. The 2D diffraction patterns consisted of pairs of well defined Bragg maxima that could be indexed to the YAG and GGG cubic lattices. No evidence of textured polycrystalline films (producing diffraction maxima spread along loci of constant d-spacing) was observed. These scattering distributions did not change significantly at any of the locations measured during the line-scan study. Further evidence of the epitaxial nature of the film was demonstrated through measurement of a series of rocking curves that focussed on the (400) YAG maxima and its associated GGG peak. Fig. 2 clearly shows diffraction peaks consistent with epitaxial growth. The film's appearance was transparent with only a slight frosty trace (for a 310 nm−750 nm thick film). Film peaks were detected at 28.7° and 59.3° (±0.05°) which correspond to the (400) and (800) GGG crystalline planes respectively [12]. The X-ray diffraction spectra were normalised to the position of the YAG (400) substrate peak of 29.806° [13]. The FWHM of the GGG (400) and (800) peaks were 0.2° and 0.5°, respectively, compared to 0.08° and 0.11° for films grown by nanosecond PLD [10]. Fig. 3 shows the X-ray diffraction spectrum of a film grown at the optimum fluence and pressure. All films grown by femtosecond PLD showed a surface morphology that was not as smooth as typical nanosecond PLD grown films, with a surface roughness value (RMS) of $60 - 70$ nm. Films with smooth surface features were not observed, whatever the growth conditions (fluence 1.3 to 19 J/cm^2, pressure 10^{-3} to 10^{-1} mbar, distance 2.5 cm to 4.5 cm). Fig. 4 shows a comparison of AFM micrographs of films of epitaxial GGG grown by femtosecond and nanosecond

PLD. This figure shows the random stacking of quasi-spherical particulates of approximately 1 μm in size for femtosecond PLD films. An SEM photomicrograph of femtosecond and nanosecond deposited films is shown in Fig. 5. The surface topography of a typical nanosecond film was considerably smoother, with a surface roughness of (RMS) $4 - 5$ nm.

The effect of each deposition parameter on the crystallinity of the femtosecond PLD grown films was investigated by X-ray diffraction analysis. Fig. 6 shows X-ray diffraction spectra for films deposited using laser fluences ranging from 1.6 J/cm^2 to 13 J/cm^2 and focal spot-sizes ranging from 45 μm by 65 μm to 137 μm by 195 μm. These results show that the optimum fluence for epitaxial growth was above 3.1 J/cm^2 and lower fluences gave rise to multi-phase growth of GGG and other anomalous phases, which have not been possible to unambiguously assign. Fig. 7 shows the XRD spectra of films grown under various temperatures. Again, films were deposited in an oxygen atmosphere of 0.1 mbar with a chosen laser fluence of 12 J/cm^2 and spot-size of 45 μm by 65 μm with a target-substrate distance of 4.5 cm. Incident CO_2 laser heating powers upon the substrate were varied from 8 W to 15.5 W, which corresponds to a temperature variation of 750 °C to 970 °C. The X-ray diffraction analysis revealed the optimum temperature for GGG growth varies between 750 °C and 900 °C. Films deposited above a temperature of 900 °C showed multi-phase growth and at a temperature of 970 °C the garnet phase of GGG was no longer evident. X-ray diffraction analysis of films deposited under various oxygen pressures, shown in Fig. 8, revealed that single crystal growth occurred preferentially at higher oxygen pressures. Lower pressures resulted in polycrystalline films dominated by the Ga-deficient phase $Gd_3(GaO_4)O_2$. At further target-substrate distances the peak position increases from 28.49° (target-

subtrate distance of 2.5 cm) to 28.63 ° (target-subtrate distance of 4.5 cm). A final investigation of the effect of the repetition rate (10 Hz to 1 kHz), using the optimum growth conditions was undertaken, however no significant difference was observed for either the crystallinity or morphology of the films.

Fig. 9 shows typical time-of-flight (TOF) spectra for femtosecond (0.82 J/cm^2) and nanosecond (0.92 J/cm^2) ablated ions in a vacuum ($< 1.6 \times 10^{-4}$ mbar). The corresponding velocity distributions are also shown. We have assumed the ions to be singly charged for our analysis, which has been confirmed by other reports of femtosecond ablation of Ti and Si for intensities similar to those used in the current study ($\sim 10^{14}$ W/cm^2) [14–16]. The main features of our results are the high velocities of the femtosecond ablated ions and the double-peak velocity distribution (observed only at low fluences). The results reveal a higher velocity ion population travelling ahead of the majority of the plume at a velocity of $\sim 1.2 \times 10^5$ m/s (peak TOF). At higher fluences (>1 J/cm^2), where ion velocities range up to $\sim 4 \times 10^5$ m/s, dual-peak distributions are less defined, which we believe is due to electrical signal oscillations as a result of rapid ion flux increases at these fluences. The most probable velocity (the velocity of the ions at the peak of TOF) for nanosecond and femtosecond ablated ions are shown in table 1.

4 Conclusions

We have demonstrated heteroepitaxial growth of Nd:GGG on YAG by femtosecond PLD and analysed the plume characteristics by the Langmuir probe technique for both nanosecond and femtosecond ablation. By systematic analysis via X-ray diffraction for films grown under various deposition parameters,

we have found the conditions necessary for epitaxial growth. The topography of the films remains poor however, revealing a comparatively rough surface. This may be due to the presence of high-energy ions changing the conditions necessary for monolayer growth on the surface of the film, or damage to the growing film from high energy ion bombardment, which generates defects and thus disturbs the smooth growth that takes place under the comparatively less energetic nanosecond regime. Conditions for monolayer growth by femtosecond PLD, which match or better the quality of nanosecond deposited films, have not yet been found. Further studies of femtosecond deposition through variation of wavelength and pulse duration are possible, and it may well be shown that further improvements can be obtained.

Figure captions

Figure 1: Probe circuit used for Langmuir probe measurements of femtosecond ablated ions.

Figure 2: Rocking curve analysis showing the GGG (400) and YAG (400) peaks. The 2-theta data is measured at systematically increasing incident angles (omega). The non-circular shape of the contour distribution is due to incident beam divergence.

Figure 3: X-ray diffraction spectrum of a film grown by femtosecond PLD with the growth conditions: fluence 19 J/cm^2; spot-size 32 μm by 45 μm; energy per pulse 0.85 mJ; target-substrate distance 4.5 cm; pressure 0.1 mbar and temperature 850 °C. The duration of the deposition was 120 minutes. The thicknesses were measured to be between a minimum and maximum of 310 nm

and 750 nm.

Figure 4: AFM micrographs of a film of epitaxial GGG deposited using a) nanosecond PLD grown film (with the conditions: fluence 2 J/cm^2; spot-size 2 mm by 5 mm; energy per pulse 200 mJ; repetition rate 10 Hz; duration 40 minutes; target-substrate distance 4.5 cm; oxygen pressure 2×10^{-2} mbar and temperature 800 °C) and b) femtosecond PLD grown film (with conditions: fluence 19 J/cm^2; spot-size 32 μm by 45 μm; energy per pulse 0.85 mJ; duration 120 minutes; target-substrate distance 4.5 cm; oxygen pressure 0.1 mbar and temperature 850 °C).

Figure 5: SEM micrographs of a film of epitaxial GGG deposited using a) nanosecond PLD b) femtosecond PLD.

Figure 6: X-ray diffraction spectra from GGG films deposited with a laser fluence (and spot-size) of a) 13 J/cm^2 (45 μm by 65 μm), b) 9.1 J/cm^2 (56 μm by 75 μm), c) 3.1 J/cm^2 (90 μm by 135 μm) d) 1.6 J/cm^2 (123 μm by 195 μm), with energy per pulse 1.2 mJ, repetition rate 1 kHz, duration 10 minutes, target-substrate distance 4.5 cm; oxygen pressure 0.1 mbar; substrate temperature 850 °C. Film thicknesses were measured to be a) $80 - 120$ nm; b) $80 - 130$ nm; c) $40 - 70$ nm; d) $60 - 70$ nm.

Figure 7: X-ray diffraction spectra of films grown at substrate temperatures of a) 750 °C b) 820 °C c) 900 °C d) 970 °C, with laser fluence 12 J/cm^2, spot-size 45 μm by 65 μm, energy per pulse 1.1 mJ, duration 10 minutes, target substrate distance 4.5 cm, oxygen pressure 0.1 mbar and temperature 850 °C. All films were between $60 - 100$ nm in thickness.

Figure 8: X-ray diffraction spectra from GGG films deposited under an oxygen pressure of a) 0.1 mbar; b) 10^{-1} mbar; c) 10^{-2} mbar; d) 10^{-3}mbar (peaks identified) with a laser fluence 6.2 Jcm^2, spot-size 65 μm by 95 μm, energy per pulse 1.2 mJ, repetition rate 1 kHz, duration 10 minutes, target-substrate distance 3 cm; and substrate temperature of 850 °C. Film thicknesses were measured to be a) 0.6 μm - 2.0 μm; b) 0.6 μm - 2.5 μm; and c) 0.6 μm - 2.5 μm.

Figure 9: TOF spectra and corresponding velocity distributions of femtosecond (a and b) and nanosecond ablated ions (c and d) in a vacuum for similar laser fluences (femtosecond 0.82 J/cm^2, nanosecond 0.92 J/cm^2).

Table captions

Table 1: Comparison of peak velocities of femtosecond and nanosecond ablated ions for similar laser fluences.

Acknowledgments

The authors wish to express their thanks to Peter Wright and QinetiQ for their support towards this work. For help and support with SEM, XRD the authors wish to thank Zondy Webber, Barbara Cressey and Mark Weller from the University of Southampton.

References

[1] R. W. Eason. *Pulsed Laser Deposition of Thin Films: Applications-Led Growth of Functional Materials*. John Wiley & Sons Inc, 2006.

[2] A. V. Rode, A. Zakery, M. Samoc, R. B. Charters, E. G. Gamaly, and B. Luther-Davies. Laser-deposited As_2S_3 chalcogenide films for waveguide applications. *APPLIED SURFACE SCIENCE*, 197:481–485, 2002.

[3] A. V. Rode, B. Luther-Davies, and E. G. Gamaly. Ultrafast ablation with high-pulse-rate lasers. Part II: Experiments on laser deposition of amorphous carbon films. *JOURNAL OF APPLIED PHYSICS*, 85(8):4222–4230, 1999.

[4] E. Millon, J. Perriere, R. M. Defourneau, D. Defourneau, O. Albert, and J. Etchepare. Femtosecond pulsed-laser deposition of $BaTiO_3$. *APPLIED PHYSICS A-MATERIALS SCIENCE & PROCESSING*, 77(1):73–80, 2003.

[5] T. W. Trelenberg, L. N. Dinh, C. K. Saw, B. C. Stuart, and M. Balooch. Femtosecond pulsed laser ablation of GaAs. *APPLIED SURFACE SCI-*

ENCE, 221(1-4):364–369, 2004.

[6] M. Womack, M. Vendan, and P. Molian. Femtosecond pulsed laser ablation and deposition of thin films of polytetrafluoroethylene. *APPLIED SURFACE SCIENCE*, 221(1-4):99–109, 2004.

[7] B. C. Stuart, M. D. Feit, S. Herman, A. M. Rubenchik, B. W. Shore, and M. D. Perry. Nanosecond-to-femtosecond laser-induced breakdown in dielectrics. *Physical Review B*, 53(4):1749–1761, January 1996.

[8] P. P. Pronko, P. A. VanRompay, C. Horvath, F. Loesel, T. Juhasz, X. Liu, and G. Mourou. Avalanche ionization and dielectric breakdown in silicon with ultrafast laser pulses. *PHYSICAL REVIEW B*, 58(5):2387–2390, 1998.

[9] E. G. Gamaly, A. V. Rode, B. Luther-Davies, and V. T. Tikhonchuk. Ablation of solids by femtosecond lasers: Ablation mechanism and ablation thresholds for metals and dielectrics. *PHYSICS OF PLASMAS*, 9(3):949–957, 2002.

[10] T. C. May-Smith, C. Grivas, D. P. Shepherd, R. W. Eason, and M. J. F. Healy. Thick film growth of high optical quality low loss ($0.1\,\mathrm{dBcm}^{-1}$) Nd:$Gd_3Ga_5O_{12}$ on $Y_3Al_5O_{12}$ by pulsed laser deposition. *APPLIED SURFACE SCIENCE*, 223(4):361–371, 2004.

[11] T. C. May-Smith, A. C. Muir, M. S. B. Darby, and R. W. Eason. ZnSe tetra-prism for homogeneous substrate heating with a CO_2 laser in pulsed laser deposition. *Submitted to APPLIED OPTICS*, 2007.

[12] H. Sawada. Electron density study of garnets: $Z_3Ga_5O_{12}$; Z = Nd, Sm, Gd, Tb. *JOURNAL OF SOLID STATE CHEMISTRY*, 132(2):300–307, 1997.

[13] L. Dobrzycki, E. Bulska, D. A. Pawlak, Z. Frukacz, and K. Wozniak. Structure of YAG crystals doped/substituted with erbium and ytterbium.

Inorganic Chemistry, 43(24):7656–7664, November 2004.

[14] O. Albert, S. Roger, Y. Glinec, J. C. Loulergue, J. Etchepare, C. Boulmer-Leborgne, J. Perriere, and E. Millon. Time-resolved spectroscopy measurements of a titanium plasma induced by nanosecond and femtosecond lasers. *Applied Physics A-Materials Science & Processing*, 76(3):319–323, March 2003.

[15] S. Amoruso, C. Altucci, R. Bruzzese, C. de Lisio, N. Spinelli, R. Velotta, M. Vitiello, and X. Wang. Study of the plasma plume generated during near IR femtosecond laser irradiation of silicon targets. *Applied Physics A-Materials Science & Processing*, 79(4-6):1377–1380, September 2004.

[16] M. Q. Ye and C. P. Grigoropoulos. Time-of-flight and emission spectroscopy study of femtosecond laser ablation of titanium. *Journal Of Applied Physics*, 89(9):5183–5190, May 2001.

Figure 1

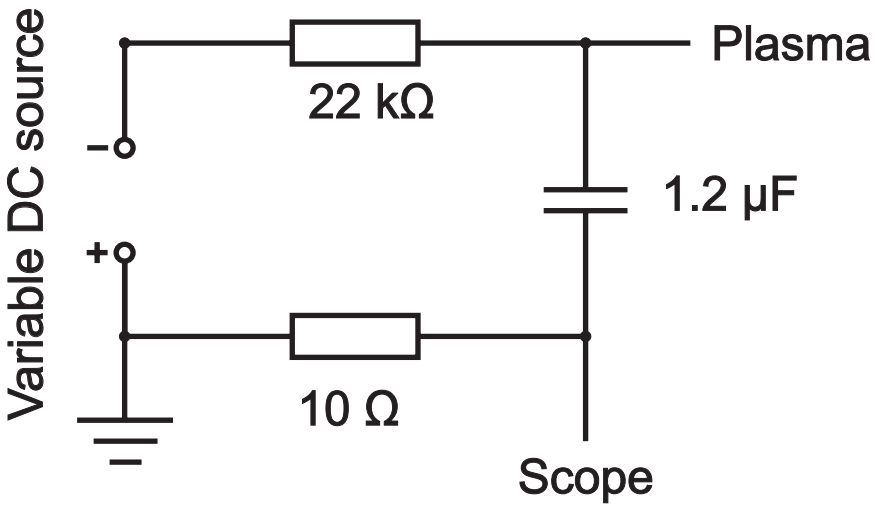

Figure 2

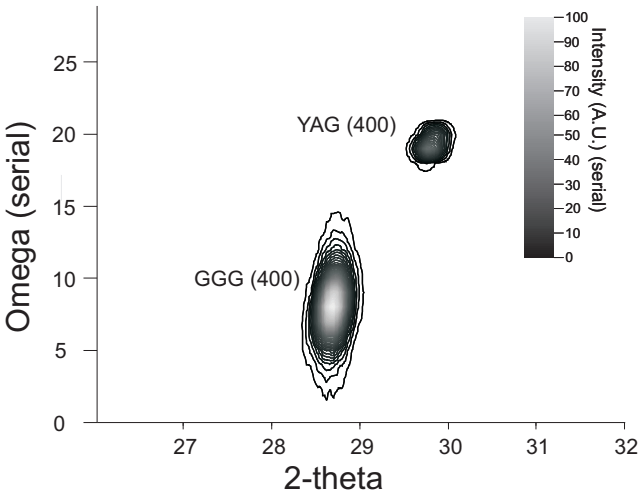
Omega (serial)
2-theta
Intensity (A.U.) (serial)
YAG (400)
GGG (400)
0
5
10
15
20
25
27
28
29
30
31
32
100
90
80
70
60
50
40
30
20
10
0

Figure 3

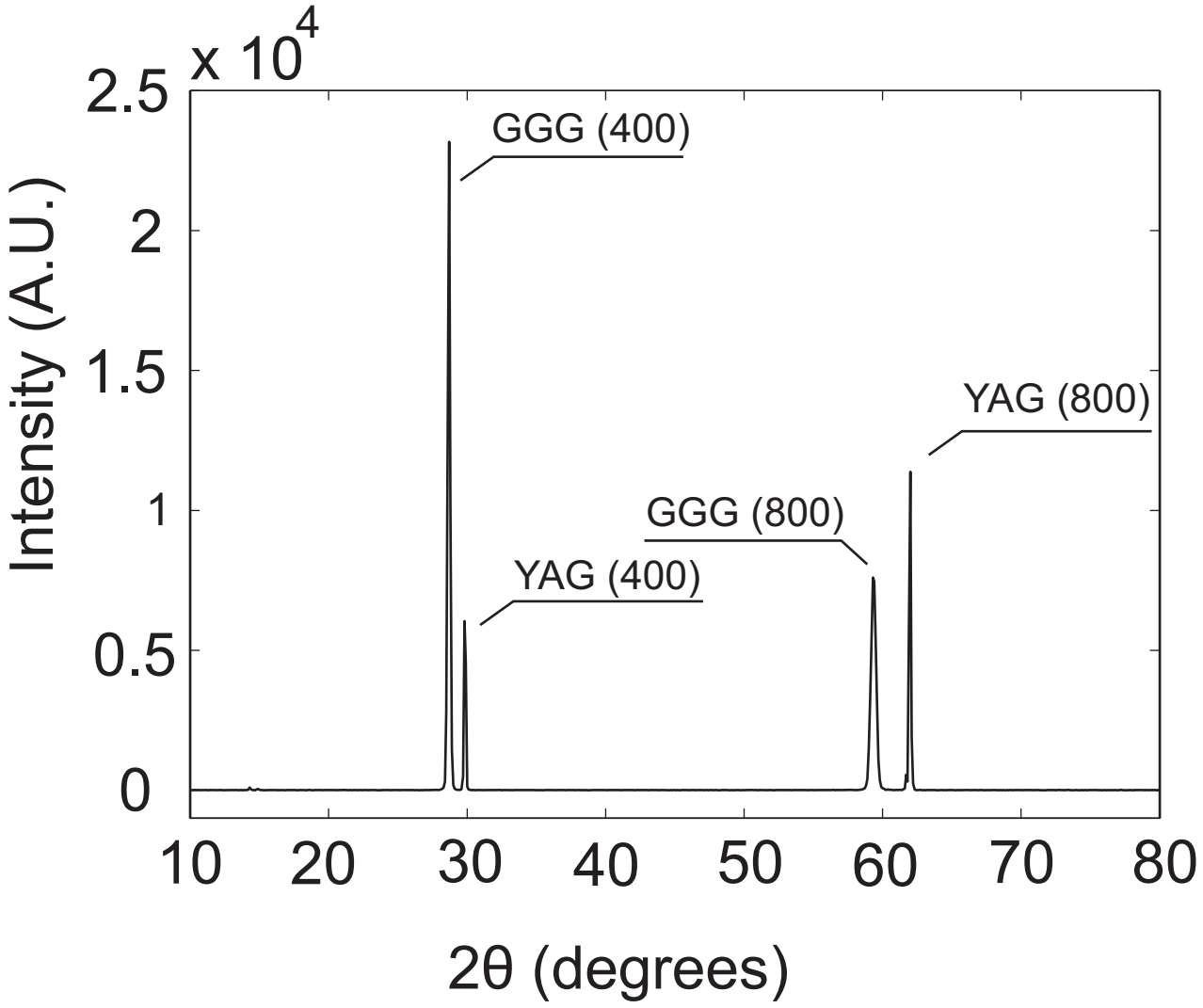
x 10^4
2.5
2
1.5
1
0.5
0
Intensity (A.U.)
GGG (400)
YAG (400)
GGG (800)
YAG (800)
10
20
30
40
50
60
70
80
2θ (degrees)

Figure 4

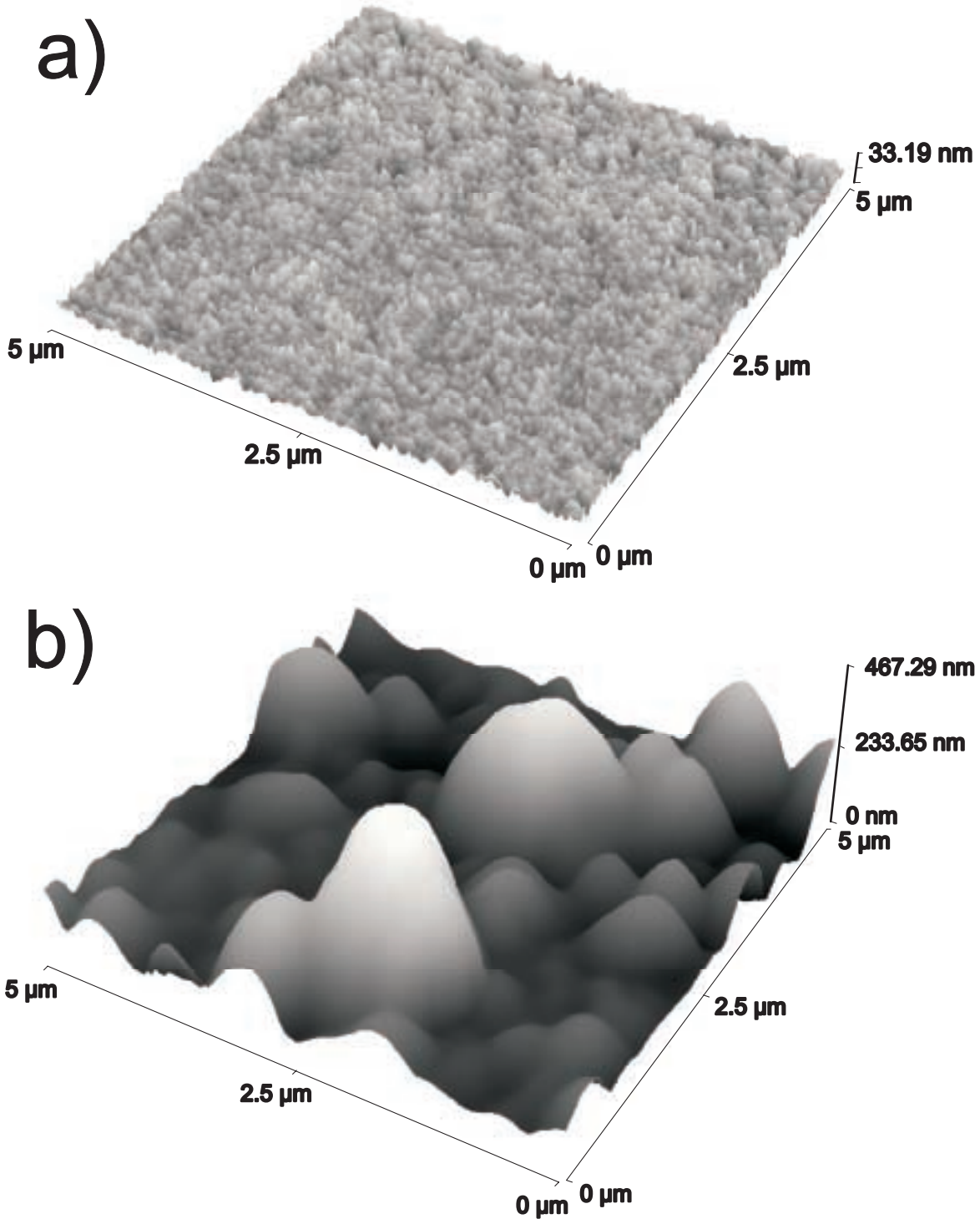
a)
33.19 nm
5 µm
5 µm
2.5 µm
2.5 µm
0 µm
0 µm
b)
467.29 nm
233.65 nm
0 nm
5 µm
5 µm
2.5 µm
2.5 µm
0 µm
0 µm

Figure 5

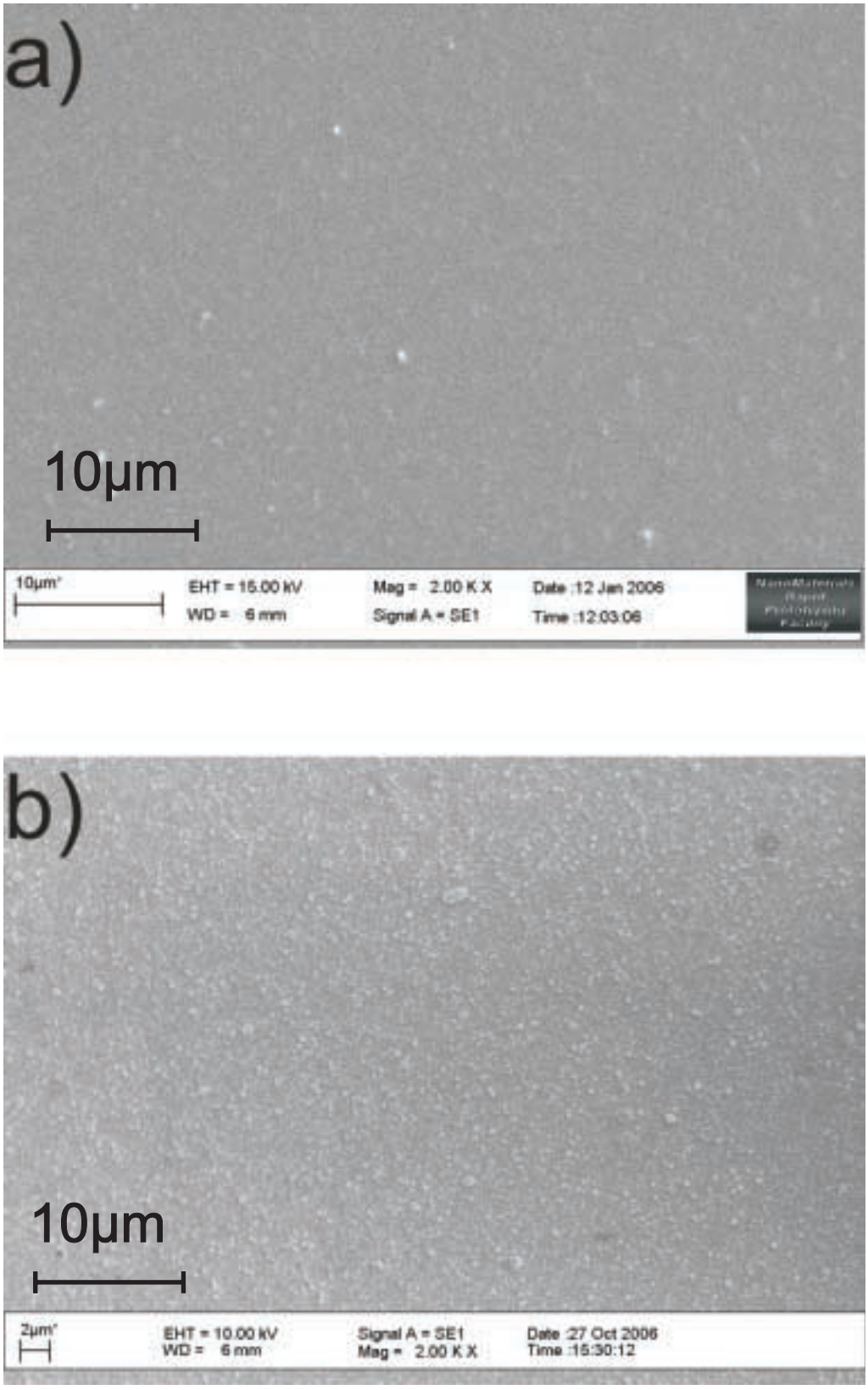
a)
10µm
10µm
EHT = 15.00 kV
WD = 6 mm
Mag = 2.00 K X
Signal A = SE1
Date :12 Jan 2006
Time :12:03:06
b)
10µm
2µm
EHT = 10.00 kV
WD = 6 mm
Signal A = SE1
Mag = 2.00 K X
Date :27 Oct 2006
Time :15:30:12

Figure 6

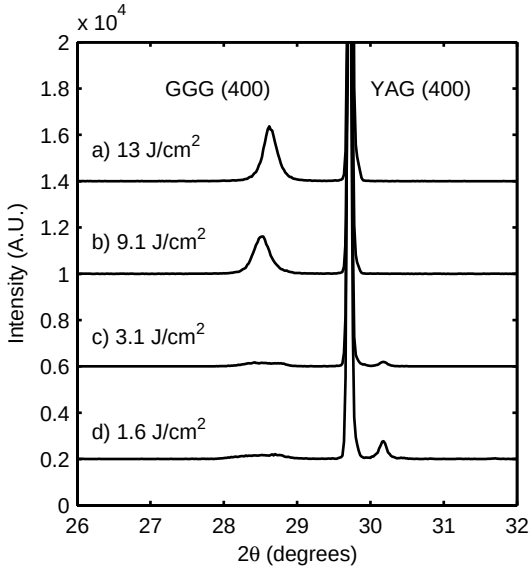
x 10^4
2
1.8
1.6
1.4
1.2
1
0.8
0.6
0.4
0.2
0
Intensity (A.U.)
GGG (400)
YAG (400)
a) 13 J/cm^2
b) 9.1 J/cm^2
c) 3.1 J/cm^2
d) 1.6 J/cm^2
26
27
28
29
30
31
32
2θ (degrees)

Figure 7

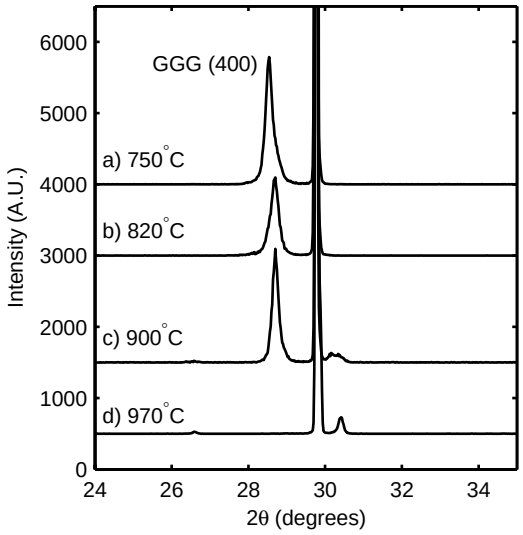
GGG (400)
a) 750°C
b) 820°C
c) 900°C
d) 970°C
Intensity (A.U.)
2θ (degrees)
0
1000
2000
3000
4000
5000
6000
24
26
28
30
32
34

Figure 8

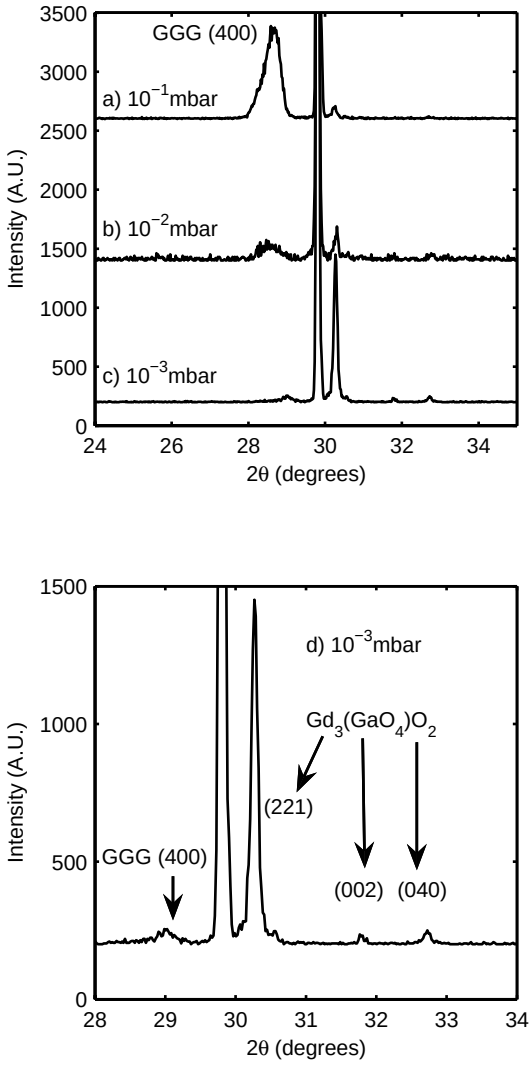
GGG (400)
a) 10^{-1}mbar
b) 10^{-2}mbar
c) 10^{-3}mbar
Intensity (A.U.)
2θ (degrees)
d) 10^{-3}mbar
Gd$_3$(GaO$_4$)O$_2$
(221)
GGG (400)
(002)
(040)
Intensity (A.U.)
2θ (degrees)

Figure 9

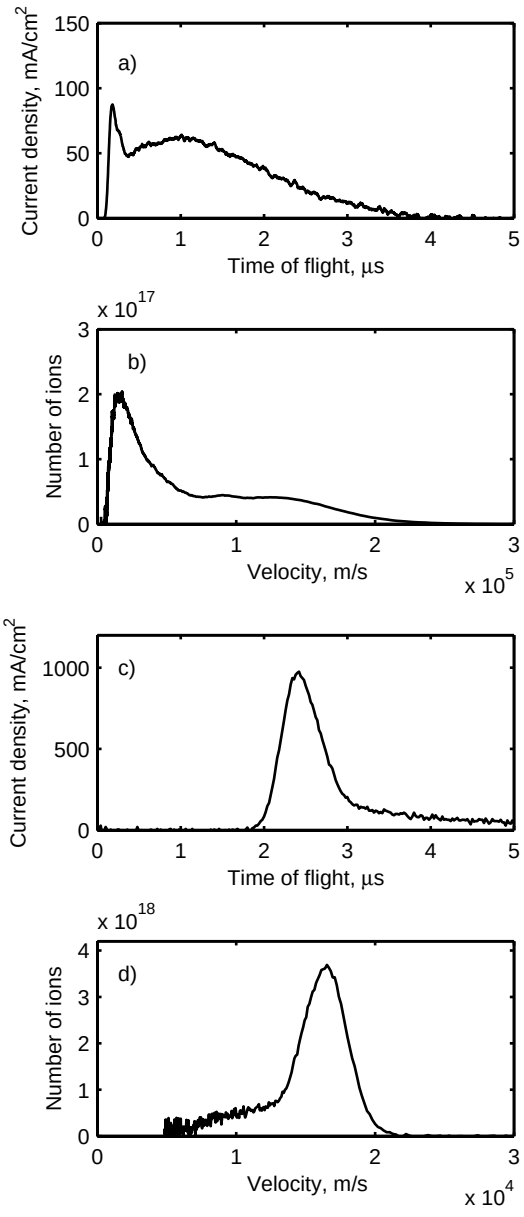
Current density, mA/cm2
150
100
50
0
a)
0
1
2
3
4
5
Time of flight, μs
x 10^17
3
2
1
0
b)
Number of ions
0
1
2
3
Velocity, m/s
x 10^5
Current density, mA/cm2
1000
500
0
c)
0
1
2
3
4
5
Time of flight, μs
x 10^18
4
3
2
1
0
d)
Number of ions
0
1
2
3
Velocity, m/s
x 10^4

Table 1

Plasma parameters	Nanosecond PLD (0.92 J/cm^2)	Femtosecond PLD (0.82 J/cm^2)
Peak velocity	1.6×10^4 m/s	1.3×10^5 m/s (fast ions) 1.8×10^4 m/s (slow ions)